JACS
JOURNAL OF THE AMERICAN CHEMICAL SOCIETY

Communication

pubs.acs.org/JACS

A New Class of Lithium and Sodium Rechargeable Batteries Based on Selenium and Selenium−Sulfur as a Positive Electrode

Ali Abouimrane,*[,†] Damien Dambournet,[†] Karena W. Chapman,[‡] Peter J. Chupas,[‡] Wei Weng,[†] and Khalil Amine*[,†]

[†]Chemical Sciences and Engineering Division, Argonne National Laboratory, Argonne, Illinois 60439, United States

[‡]X-ray Science Division, Advanced Photon Source, Argonne National Laboratory, Argonne, Illinois 60439, United States

Supporting Information

ABSTRACT: A new class of selenium and selenium−sulfur (Se_xS_y)-based cathode materials for room temperature lithium and sodium batteries is reported. The structural mechanisms for Li/Na insertion in these electrodes were investigated using pair distribution function (PDF) analysis. Not only does the Se electrode show promising electrochemical performance with both Li and Na anodes, but the additional potential for mixed Se_xS_y systems allows for tunable electrodes, combining the high capacities of S-rich systems with the high electrical conductivity of the *d*-electron containing Se. Unlike the widely studied Li/S system, both Se and Se_xS_y can be cycled to high voltages (up to 4.6 V) without failure. Their high densities and voltage output offer greater volumetric energy densities than S-based batteries, opening possibilities for new energy storage systems that can enable electric vehicles and smart grids.

The discovery of new electrode materials is key to realizing safe and efficient electrochemical energy storage systems essential to enabling future green energy technologies.[1−4] Beyond conventional intercalation chemistry,[5] reaction of lithium with sulfur[6−8] and oxygen[9−11] (so-called "Li-air" batteries) have the potential to provide 2 to 5 times the energy density of current commercial systems. However, both Li/S and Li/O_2 systems suffer from cycling performance issues that impede their commercial applications: Li/O_2 cycling is limited by electrolyte decomposition and large cell polarization; Li/S suffers from the low conductivity of S and the solubility of intermediary polysulfide species during cycling.

Here we explore the potential of selenium, a *d*-electron containing member of group 16 with high electrical conductivity, as an electrode material for rechargeable batteries. We show that Se and mixed Se_xS_y represent an attractive new class of cathode materials with promising electrochemical performance in reactions with both Li and Na ions. Notably, unlike existing Na/S batteries that only operate at high temperature, these new Se and Se_xS_y electrodes are capable of room temperature cycling against Na. Accordingly, Se not only provides opportunities for developing new high performance rechargeable batteries, including mixed chalcogenide-systems but also has the potential to enhance our fundamental understanding of batteries.

The redox reactions of carbon nanotube-containing composite Se and SeS_2 electrodes (Se−C and SeS_2−C), with metallic Li and Na, were investigated within a coin cell. Details of material and cathode preparation and cell assembly are provided in the Supporting Information (SI). The electrochemical characteristics of the Se-based electrode are shown in Figure 1. For reactions with both Li and Na, the capacity of the first discharge corresponds to the complete reduction of the selenium: $Se + 2A^+ + 2e^- \leftrightarrow A_2Se$ (A = Li, Na). The shape of the voltage profile provides insight into the structural mechanism for these reactions. For Li/Se−C, the initial discharge (Li insertion) involves one well-defined plateau (at 2 V) indicative of a single phase transition. This single phase transition is consistent with the existence of only one Li−Se phase (i.e., Li_2Se). For Na/Se−C, the discharge involves two plateaus: a short one at 1.9 V and a longer one at 1.5 V. This suggests that the full discharge product (Na_2Se) is formed *via* an intermediate phase. During the ensuing charge (Se oxidation), both Li/Se−C and Na/Se−C show two plateaus (at 2.4 and 3.75 V, and 2.1 and 3.5 V, respectively). For both Li and Na, the apparent total charge capacity exceeded that of the discharge which may suggest a partial dissolution of the soluble Li_nA ($n < 2$) electrode—a "redox shuttle" effect.[12] During the early cycles, the Li/Se−C voltage profile becomes more complex, with increases in the charge and discharge potentials. Beyond ∼5 cycles, the charge potential stabilizes at ∼3.7 V, while the average discharge potential increases to ∼2.5 V.

Repeated cycling, up to 100 cycles, demonstrates the excellent cycle life of these systems (Figure 1). The Li/Se−C system sustained a reversible capacity of ∼500 mAh g^{-1} for >25 cycles at low current density (10 mA g^{-1}, ∼C/60), which reduced to ∼300 mAh g^{-1} at higher current density (50 mA g^{-1}, ∼C/12) with a small fade for 100 cycles. For Na/Se−C, a lower capacity was observed with an excellent cycle life (265 mAh g^{-1} at 50 mA g^{-1}).

To gain insight into the structural mechanisms underlying the Li and Na insertion reaction, high-energy X-ray scattering data, suitable for pair distribution function (PDF) analysis, were obtained for samples recovered from various states of charge and discharge. Data were collected at beamline 11-ID-B at the Advanced Photon Source at Argonne National Laboratory. The PDF provides local and long-range structural information as a

Received: December 16, 2011
Published: February 25, 2012

dx.doi.org/10.1021/ja211766q | *J. Am. Chem. Soc.* 2012, 134, 4505−4508

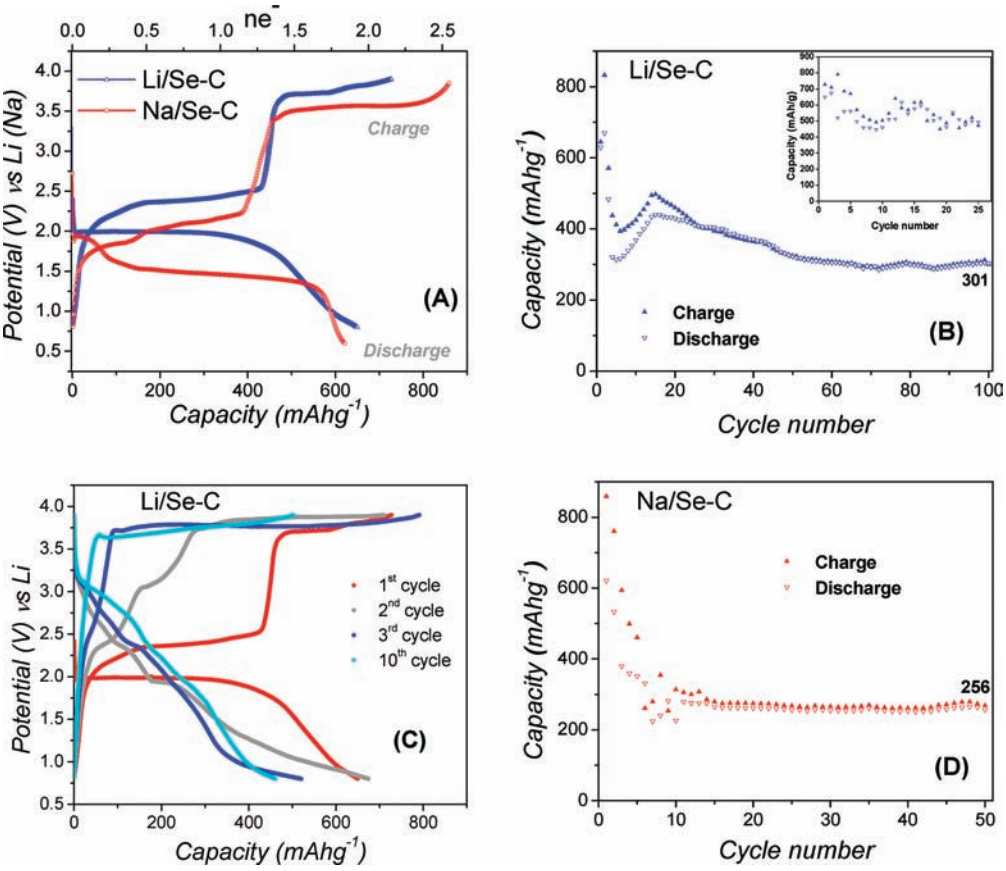

Figure 1. Voltage profiles for Li/Se−C and Na/Se−C during the first discharge/charge (a) and for Li/Se−C during selected cycles (c). The capacity retention of Li/Se−C (b) and Na/Se−C (d) cycled at 50 and 10 mA g^{-1} (inset) current density.

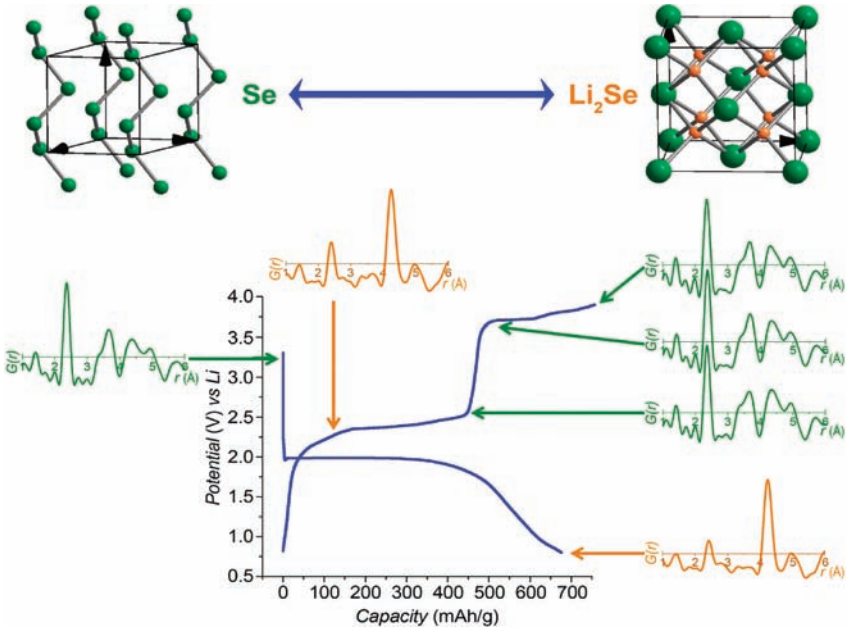

Figure 2. PDFs for the pristine Se−C electrode and upon recovery from various states of discharge/charge. Structural representations of the Se and A_2Se (antifluorite) phases are shown.

histogram of all atom−atom distances within a system, independent of crystallinity.[13] Unlike conventional diffraction methods, it allows phases to be identified regardless of any changes in particle size (including nanoscale particles), particle morphology, or structural order. PDFs of the pristine and recovered Li/Se−C materials are shown in Figure 2. Refinement of a structure against the data obtained for pristine Se confirmed the trigonal structure, with chains of Se atoms linked by Se−Se bonds of 2.36 Å. Fits to the data for the fully discharged material confirm the formation of an antifluorite-

dx.doi.org/10.1021/ja211766q | J. Am. Chem. Soc. 2012, 134, 4505−4508

type Li_2Se phase. At intermediate points in the discharge (2 V, ~240 mA g^{-1}), both Li_2Se and Se are present, in agreement with the occurrence of a single, first-order phase transition. Insertion of Na induced a dramatic broadening of the peaks in the PDF (at 1.4 V, ~350 mAh g^{-1}, ~1 Na per Se) (Figure S5), suggesting the formation of a poorly ordered intermediate (likely during the plateau at 2.0 V), before transforming to a well-defined antifluorite-type Na_2Se phase upon complete discharge.[14]

During the first charge (reoxidation), the PDF data show that the first plateau (e.g., at ~2.3 V for Li/Se−C) corresponds to the conversion of A_2Se to Se, while the second plateau (at 3.75 V) is associated with minimal structural changes to the electrode. This indicates that the second plateau is not associated with an electrochemical reaction of the cathode. Instead it is consistent with a redox shuttle effect, whereby Li/Na polyselenide species, formed during the charge dissolve in the electrolyte, migrate to the anode, react with the Li/Na, and return to the cathode, thereby producing additional capacity. This is known for Li/S systems and leads to a disparity between the charge and discharge capacities, that is, low efficiency.

The features of the voltage profiles evolve with cycling, with the most significant changes during the first 3 cycles. For Li/Se−C, the plateau at 2.3 V during charge is less clearly defined in the second cycle, and PDF data indicate that Li_2Se persists to higher potentials than during the initial charge, with both Li_2Se and Se phases present at 3.0 V. In the third charge, the reaction again shifts to higher potential, with a single plateau at ~3.6 V (where it stabilizes for subsequent cycles) corresponding to the oxidation of Li_2Se to Se. Similar trends are observed for the Na/Se−C system. This evolution of the voltage profiles may be associated with changes to the electrode microstructure upon cycling.[15] Indeed, PDFs of samples subjected to 3 discharge−charge cycles are broadened as is consistent with increased disorder (Figure S7). A small capacity fade evident for Li/Se−C but not Na/Se−C during later cycles (cycles 20−40, 50 mA g^{-1} current density) could reflect continuing minor changes in microstructure or differences in the polyselenide solubility.

The disparity between the charge and discharge capacities—the redox shuttle effect—progressively diminishes with increasing cycling (Figure 1). At 50 mA g^{-1} current density, this effect is entirely eliminated after ~15 cycles for Na/Se−C and ~20 cycles for Li/Se−C. At lower current densities, this redox shuttle effect is eliminated earlier.

Extension of the cycling potential up to 4.6 V did not adversely impact the electrochemical performance of Li/Se−C, which sustains a capacity of 280 mAh g^{-1} over 80 cycles (100 mA g^{-1}, ~C/6, Figure 3). Importantly, this allows for use of high potential windows, unlike for Li/S, where charging beyond 3.6 V disables any further cycling.[16]

The Se-containing electrodes provide several advantages over widely studied S systems:

(1) Se has higher electric conductivity, approximately 20 orders of magnitude greater than S (10^{-5} S cm^{-1}; cf. 5 $\times 10^{-30}$ S cm^{-1}). This facilitates cycling with Na at room temperature, while Na/S operation is limited to elevated temperatures (300−350 °C).

(2) The redox shuttle effect seems more limited for Se. We anticipate that strategies applied to optimize the performance of S-based systems, for example, additives, use of large quantities of carbon, carbon morphologies and the use of microporous materials that minimize redox shuttle effects,[7,8,17,18] could be extended to further enhance the performance of the Se-based systems.

(3) Despite a lower theoretical gravimetric capacity, the high density of Se allows for volumetric capacities that are comparable to S (Se: 3253 Ah L^{-1} based on 4.82 g cm^{-3}; S: 3467 Ah L^{-1} based on 2.07 g cm^{-3}).

(4) The Se systems provide higher output voltages than S and, accordingly, higher energy densities, a key advantage in commercial applications. For Li/Se, the output voltage is at least 0.5 V higher for Li/S.

(5) For Na/Se, the theoretical capacity exceeds that observed for Na/S at room temperature. Indeed, for Na/Se, PDF analysis indicates that Na_2Se forms (675 mAh g^{-1} capacity), while for the Na/S system only Na_2S_3 and Na_2S_2 are detected (558−837 mAh g^{-1} capacity).[19]

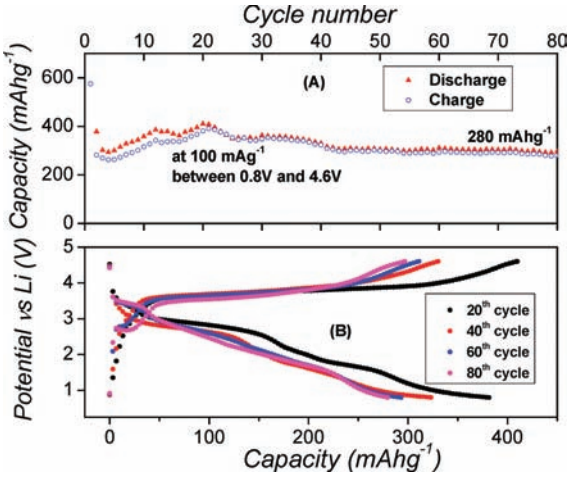

Figure 3. Cycling stability (a) and voltage profile (b) of Li/Se−C between 0.8 and 4.6 V (100 mA g^{-1} current density).

From a practical standpoint, the toxicity of Se is comparable to S and other common electrode elements (LD50: Se ~6.2 g; S ~8.4 g; Co ~6.7 g; Ni ~5.0 g), and it is included, in trace quantities, in supplements and personal care items. While the lower abundance (and higher cost) of Se compared to S may impede large scale commercialization, this could be largely offset by using Na rather than Li, and/or by using mixed Se_xS_y systems.

Preliminary investigation of one mixed chalcogenide system, SeS_2−C (Figure 4), demonstrates that Se_xS_y-based electrodes can offer higher theoretical capacities than the Se alone, with improved performance and conductivity compared to S. For Li/SeS_2−C, the discharge capacity is 30% greater than Li/Se−C in the range 0.8 to 4.6 V (512 vs 394 mAh g^{-1} after 30 cycles, 50 mA g^{-1} current density). As for the pure Se-system, SeS_2−C can be cycled with Na at room temperature, with a capacity of 288 mAh g^{-1} sustained over 30 cycles. As Se and S are infinitely miscible,[20] with many readily available solid solutions (e.g., Se_5S, Se_5S_2, Se_5S_4, SeS, Se_3S_5, SeS_2, SeS_7),[21] Se_xS_y materials represent a broad class of new battery electrodes with higher theoretical capacities than Se alone (675−1550 mAh g^{-1} for systems above) with improved conductivity (and room temperature cycling) compared to S alone (see SI). Systems with even lower Se proportions, i.e. SeS_{20}, can be easily prepared.

In the current drive to discover and optimize materials for electrochemical energy storage, this new class of room temperature Li- and Na-based Se_xS_y rechargeable batteries

dx.doi.org/10.1021/ja211766q | J. Am. Chem. Soc. 2012, 134, 4505−4508

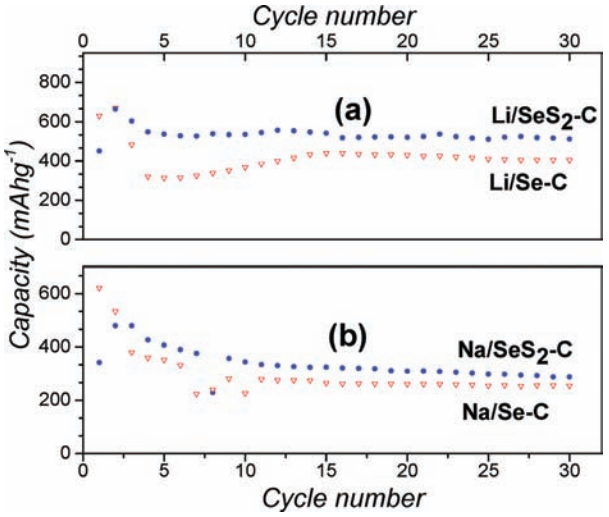

Figure 4. Cycling performance of Li/SeS_2−C, Li/Se−C, Na/SeS_2−C, and Na/Se−C systems.

paves the way for new, promising opportunities to enable high energy batteries for transportation and grid applications.

■ ASSOCIATED CONTENT

Supporting Information

Details of composite electrode preparation, experimental procedures and PDF analysis. This material is available free of charge via the Internet at http://pubs.acs.org.

■ AUTHOR INFORMATION

Corresponding Author

Abouimrane@anl.gov; amine@anl.gov

Notes

The authors declare no competing financial interest.

■ ACKNOWLEDGMENTS

The authors thank Dr. Nancy Dietz for SEM measurements. This work was funded by the U.S. Department of Energy, Vehicle Technologies Office. Work done at Argonne and use of the Advanced Photon Source, an Office of Science User Facility operated for the U.S. Department of Energy (DOE) Office of Science by Argonne National Laboratory under Contract No. DE-AC02-06CH11357. Some electron microscopy measurements were accomplished at the Electron Microscopy Center for Materials Research at Argonne National Laboratory.

■ REFERENCES

(1) Armand, M.; Tarascon, J.-M. *Nature* **2008**, *451*, 652.
(2) Chung, S.-Y.; Bloking, J. T.; Chiang, Y.-M. *Nat. Mater.* **2002**, *1*, 123.
(3) Kang, K.; Meng, Y. S.; Breger, J.; Grey, C. P.; Ceder, G. *Science* **2006**, *311*, 977.
(4) Tarascon, J. M. *Philos. Trans. R. Soc. London, Ser. A* **2010**, 368.
(5) Whittingham, M. S *Science* **1976**, *192*, 1126.
(6) Rao, M. L.B. *Organic electrolyte cells*, U.S. Patent, 3,413,154, November 26, 1968.
(7) Ji, X.; Lee, K. T.; Nazar, L. F. *Nat. Mater.* **2009**, *8*, 500.
(8) Zhang, B.; Qin, X.; Li, G. R.; Gao, X. P. *Energy Environ. Sci.* **2010**, *3*, 1531.
(9) Abraham, K. M; Jiang, Z. A *J. Electrochem. Soc.* **1996**, *143*, 1.
(10) Ogasawara, T.; Debart, A.; Holzapfel, M.; Novak, P.; Bruce, P. G. *J. Am. Chem. Soc.* **2006**, *128*, 1390.
(11) Read, J. *J. Electrochem. Soc.* **2002**, *149*, 1190.
(12) Rao, B. M. L.; Shrophire, J. A. *J. Electrochem. Soc.* **1981**, *128*, 942.
(13) Egami, T.; Billinge, S. J. L. In *Underneath the Bragg Peaks: Structural Analysis of Complex Materials*; Cahn, R., Ed.; Pergamon Press: Oxford, U.K., 2004.
(14) Such differences can be explained by a richer phase diagram for Na−Se compared to Li−Se. Indeed, there is only one intermediate Li−Se phase (Li_2Se), but there are many Na−Se intermediate phases including Na_2Se, Na_2Se_2, Na_2Se_3, Na_2Se_4, and Na_2Se_6. See: Sangster, J.; Pelton, A. D. *J. Phase Equilib.* **1997**, *18*, 185.
(15) Delmer, O.; Balaya, P.; Kienle, L.; Maier, J. *Adv. Mater.* **2008**, *20*, 501.
(16) He, X.; Pu, W.; Ren, J.; Wang, L.; Wang, J.; Jiang, C.; Wan, C. *Electrochim. Acta* **2007**, *52*, 7372.
(17) Aurbach, D.; Pollak, E.; Elazari, R.; Salitra, G.; Kelley, C. S.; Affinito, J. *J. Electrochem. Soc.* **2009**, *156*, A694.
(18) Demir-Cakan, R.; Morcrette, M.; Nouar, F.; Davoisne, C.; Devic, T.; Gonbeau, D.; Dominko, R.; Serre, C.; Férey, G.; Tarascon, J.-M. *J. Am. Chem. Soc.* **2011**, *133*, 16154.
(19) Ryu, H.; Kim, T.; Kim, K.; Ahn, J.; Nam, T.; Wang, G.; Ahn, H. *J. Powers Sources* **2011**, *196*, 5186.
(20) Hansen, P. M.; Anderko, K. *Construction of Binary Alloys*; : New York, 1958; p 1162.
(21) Kotkata, M. F.; Nouh, S. A.; Farkas, L.; Radwan, M. M. *J. Mat. Sci.* **1992**, *27*, 1785.